Concentration Regimes in Solutions of Polyelectrolyte Stars

N. P. Shusharina and M. Rubinstein*

Department of Chemistry, University of North Carolina, Chapel Hill, North Carolina 27599-3290

Received May 21, 2007; Revised Manuscript Received October 21, 2007

ABSTRACT: We present a scaling theory for solutions of star-branched polyelectrolytes in different concentration regimes. We distinguish between two cases of counterion distribution around the star arms and describe differences in the structure of stars with and without counterions condensed on the arms. Above the overlap concentration c^*, the size of stars decreases with increasing concentration in such a way that the stars remain at the onset of overlap in a wide range of concentrations. This regime of compaction (which we call the overlap regime) continues until the length of the star arms decreases either to the value determined mainly by the intra-arm repulsion or to the Gaussian size of a linear chain in a semidilute solution. At higher concentrations, stars interdigitate and the solution structure resembles that of a semidilute solution of linear chains. Added salt screens the electrostatic interactions within the star if salt concentration is higher than the concentration of counterions which are not condensed on the arms.

1. Introduction

Polymers with a star-branched architecture constitute a very important class of macromolecules. Dilute solution properties of stars are similar to the properties of spherical micelles formed by block copolymers[1] and of the polymer-coated colloids.[2] Studies of the compressibility and friction between surfaces with end-grafted polymers[3] as well as flow of star solutions[4] are important for the development of advanced materials.

The uncharged polymer stars and spherical brushes have been extensively investigated both theoretically[5−7] and experimentally.[8,9] It has been established that the arms of uncharged stars in dilute solutions are stretched in comparison with equivalent linear chains. The stretching is caused by the repulsive interactions between the segments belonging to different arms. The interarm repulsion does not completely vanish above the overlap concentration c^* where the stars interact with each other. As a result, the stretching of the arms delays interpenetration of stars above c^*. Instead, the stars compact while remaining at the onset of overlap in a wide range of concentrations.[7] In the semidilute regime, the stars consist of the cores of stretched inner sections of the arms and a sea of overlapping outer sections.[7,9] The structure of the sea is the same as that of a semidilute solution of linear polymers.[10]

Stars made of polyelectrolyte chains exhibit much stronger arm stretching than neutral stars.[11−13] This stretching is caused by either the electrostatic long-range repulsion between arms or by the osmotic pressure created by the counterions confined within the volume of the star.[11] The confinement of counterions is caused by their interaction with the electric field of the star.[14] If the interaction energy of the counterions with the field is much larger than the thermal energy, a minimum of the total free energy is achieved by localization of the counterions in a vicinity of the star. The effective decrease of the charge of a star reduces the electrostatic energy at the expense of the loss of the translational entropy of counterions. The counterions within a sphere surrounding the star remain osmotically active. If the linear charge density along the arms of the star is higher than approximately one elementary charge per Bjerrum length (the distance at which the interaction between two elementary charges is on the order of the thermal energy), the counterions condense into the close vicinity of each arm and practically lose their translational entropy.[15] The condensation of counterions on the arms is typical for aqueous solutions of stars with a high fraction of charged Kuhn segments. The arms with condensed counterions are stretched weaker than in the absence of condensation. Recently, the condensation of counterions on star arms has been investigated by Monte Carlo simulations[16] and by molecular dynamics simulations combined with the variational free energy calculations.[17,18]

Screening of the electrostatic interactions within a star in concentrated solutions has been studied by the self-consistent mean-field theory. However, in the SCF approach used by the authors in ref 19, the increase of polymer concentration is modeled by a decrease of space available for one star and thus the interactions between the stars has been substituted by a confinement.

Solutions of polyelectrolyte stars in the form of spherical diblock copolymer micelles with frozen cores have been experimentally studied by Muller et. al[20] over a wide range of polymer concentration. The micellar aggregation number or the number of arms in the star was obtained from the small angle neutron scattering (SANS). The hydrodynamic radius of the whole micelle was measured in dilute solutions by dynamic light scattering. From the results of the two methods, the overlap concentration was calculated as a concentration of physical overlap of spheres with the total mass of a micelle and the total size equal to the hydrodynamic radius measured in a very dilute solution. The interaction between micelles was studied by neutron scattering in concentrated solutions. The SANS results show that there are two scattering peaks at concentrations much higher than the overlap concentration. The position of one of these peaks changes with concentration c as $c^{1/3}$, while the position of the other varies as $c^{1/2}$. The authors proposed a qualitative explanation for the appearance of the second peak. They suggested that this peak is either due to the interpenetration of the stars or due to the contraction of some arms inside the star. However, their results do not allow one to qualitatively distinguish between these two interpretations, and therefore, it is not clear whether the stars interpenetrate or remain separated.

Recent experimental studies[22,23] have demonstrated that polyelectrolyte stars do not interdigitate until the solution

* Corresponding author.

10.1021/ma0711442 CCC: $40.75 © 2008 American Chemical Society
Published on Web 12/06/2007

concentration significantly exceeds the overlap concentration. The radius of each star decreases proportionally to the distance between the centers of mass allowing more stars to be accommodated in a space-filling manner before the interdigitation begins.

Studying the effect of salt on the star structure, the authors of ref 24 were focused on the distribution of salt ions in a solution of osmotically swollen stars. They applied the Donnan equilibrium rule[25] to calculate the total ion concentration within the star. The results of their calculations confirmed by the experimental data[24,26−28] show that the effect of salt on the star radius becomes noticeable if the salt concentration c_s exceeds the concentration of counterions within the star.

Experiments[24,26] show that the stars are less sensitive to the addition of salt than planar polyelectrolyte brushes.[29,30] The reported dependencies of the stars radius on the salt concentration exhibit a plateau at low c_s followed by a power law decrease c_s^{-m} where m varies from 0.11 to 0.21.[24,26−28] The scaling theory[31,32] predicts a power law decrease of the star radius with the salt concentration with exponent $m = {}^1/_5$. The scaling model developed in refs 31 and 32 does not take into account the condensation of counterions on the arms. It is based on the assumption that the screening of the electrostatic interactions in a star solution is governed by either counterions or by salt ions and controlled by the Debye length. We distinguish between two qualitatively different effects of counterions: charge reduction and screening. The first one is an effective decrease of the net charge of a star by increasing the concentration of counterions within or near it. The effectively reduced charges can still interact by the long-range (unscreened) electrostatic repulsion. The second effect of counterions, called electrostatic screening, requires local electroneutrality and leads to screened Coulomb interactions between segments decaying exponentially on length scales longer than screening length. We show that counterions do not screen the electrostatic interactions within the star but only effectively reduce its charge and dominate the osmotic pressure both inside and outside the star. The size of the strongly stretched star is determined by the balance of the osmotic pressure of counterions inside it and the entropic elasticity of its arms in the most important low salt regime, called osmotic regime. The electrostatic interactions are screened in a solution with added salt if salt concentration exceeds the concentration of counterions.

In the present paper we use the scaling theory to calculate the diagram of concentration regimes of both salt-free and salt solutions of polyelectrolyte stars. We extend the theory presented in refs 12, 31, and 32 to the case of condensation of counterions on the star arms. For the case of no condensation, we identify a new regime where the stars compact with increasing concentration without interdigitation. For solutions with added salt, we present a clear physical picture of all regimes starting from the low salt limit where screening of electrostatic interactions is not important and ending with the regime of complete screening.

In the following section, we review the theory of counterion condensation on a linear polyelectrolyte chain in a dilute salt-free solution discussed in ref 33. In section 3 we review the theory of polyelectrolyte stars in a dilute salt-free solution, developed by Borisov,[12] and generalize it to the case of counterion condensation on star arms. In section 4 we describe the regimes of dilute and concentrated salt-free solutions of polyelectrolyte stars with and without counterion condensation on star arms. Section 5 analyzes an influence of added salt on the structure of the solutions of stars. Conclusions and discussion of our results are presented in section 6.

2. Dilute Solution of Linear Polyelectrolyte Chains

Let us consider flexible linear polymer chains consisting of N Kuhn segments of length b each. The chains are dissolved in a polar solvent (e.g., in water) with dielectric permittivity ϵ at temperature T. The non-Coulomb interactions of the segments with the solvent are assumed to be θ-like. The generalization of the theory to polyelectrolyte solutions in a good solvent is straightforward. The polymer concentration in solution is expressed in terms of the Kuhn segment number density c. A chain contains Nf charged segments, each carrying the elementary charge e. Thus the net charge of the chain is eNf and, correspondingly, there are Nf monovalent counterions per chain in the solution.[34] In sections 2−4 we discuss solutions with no added salt, while in section 5 the effect of added salt is analyzed.

Polyelectrolyte chains in dilute solutions are stretched due to the intrachain electrostatic repulsion. Conformation of a polyelectrolyte chain can be described as a linear array of electrostatic blobs (the electrostatic blob is a section of a chain having the electrostatic energy on the order of the thermal energy k_BT). If the electrostatic interactions are weaker than the thermal energy, the statistics of a section of the chain in a θ-solvent is almost Gaussian. In this case, the size of the electrostatic blob ξ_{el} is related to the number of segments g_{el} in it as $\xi_{el} \approx bg_{el}^{1/2}$. From this relation and the fact that electrostatic energy of the blob is on the order of the thermal energy

$$k_BT \approx \frac{(efg_{el})^2}{\epsilon\xi_{el}} \tag{1}$$

one can derive the size of the blob[10,35]

$$\xi_{el} \approx b(uf^2)^{-1/3} \tag{2}$$

where u is the ratio of the Bjerrum length

$$l_B = \frac{e^2}{\epsilon k_BT} \tag{3}$$

to the Kuhn segment length b, $u \equiv l_B/b$.

The length of a linear polyelectrolyte chain in a dilute solution is estimated as $R_{lin}^d \approx \xi_{el}N/g_{el}$ and it is expressed as

$$R_{lin}^d \approx \frac{b^2N}{\xi_{el}} \approx bN(uf^2)^{1/3} \tag{4}$$

The electrostatic energy of interaction of a probe elementary charge with a chain of blobs at the distance r, or the electrostatic potential of the chain, can be approximated by the potential of a charged cylinder $(e\rho_0/\epsilon)\ln r$, where

$$\rho_0 = \frac{eg_{el}f}{\xi_{el}} \approx \frac{ef^{1/3}}{bu^{1/3}} \tag{5}$$

is the linear charge density along the chain of electrostatic blobs with the size ξ_{el} each.

Counterions are attracted to the chain and can condense on it effectively neutralizing a fraction of its charge.[36] Condensed counterions are localized in the space within the blobs losing their translational entropy while reducing the effective charge of the chain. Condensation is favorable if the energy of attraction is larger than the loss of entropy associated with the confinement

of a counterion which is equal to $k_BT \ln(fcb^3)$. If the linear charge density ρ_0 is higher than one elementary charge per Bjerrum length $\rho_0 > e/l_B$, then we meet the Manning condition for condensation[15] $l_B\rho_0/e > 1$, or

$$u^2 f > 1 \tag{6}$$

If the condition (eq 6) is fulfilled, a finite fraction of counterions condenses on the chain. The fraction β of counterions remains free (osmotically active), while the fraction $1 - \beta$ condenses on the chain reducing the linear charge density down to one charge per Bjerrum length.

The chain becomes effectively weaker charged due to counterion condensation, leading to a larger size of the electrostatic blob

$$\xi_{el}^c \approx b(uf^2\beta^2)^{-1/3} \tag{7}$$

The parameter β is estimated from the condition (in the scaling model we omit logarithmic corrections)

$$\frac{e\rho}{\epsilon} \approx k_BT \tag{8}$$

where $\rho = eg_{el}^c f\,\beta/\xi_{el}^c$ is the linear charge density of the chain of blobs of the size ξ_{el}^c with the counterions condensed on it (cf. eq 5). Therefore the fraction of free counterions is

$$\beta \approx \frac{1}{u^2 f} \quad \text{for} \quad u^2 f > 1 \tag{9}$$

and the rest of the counterions (fraction $1 - \beta$) condense on the chain. The size of the electrostatic blob for a chain with condensed counterions is therefore on the order of the Bjerrum length

$$\xi_{el}^c \approx l_B \quad \text{for} \quad u^2 f > 1 \tag{10}$$

and the length of the chain is

$$R_{lin}^c \approx bNu^{-1} \quad \text{for} \quad u^2 f > 1 \tag{11}$$

The conformation of the chain in the regime of condensed counterions corresponds to the condition of one uncompensated charge per electrostatic blob ($g_{el}^c \beta f \approx 1$). In this case, both blob size and the length of the chain do not depend on the fraction of charged segments f along the chain which is replaced by the effective fraction of charged segments $\beta f \approx 1/u^2$. This indicates that the increase of the charge fraction f above u^{-2} is completely compensated by the condensed counterions (for $u^2 f > 1$). In the case of no condensation ($u^2 f < 1$), the electrostatic blob size is given by eq 2 and the chain length by eq 4.

The exact solution of the Poisson−Boltzmann equation for counterion distribution in a dilute solution of linear polyelectrolytes has been presented in ref 37. The counterion condensation discussed in the present paper corresponds to the phase II-"saturated condensation" of ref 37. We do not consider exponentially low concentrations corresponding to the phase III-"unsaturated condensation" of Deshkovski et al.[37]

In the next section we will consider conformations of a polymer star consisting of p linear polyelectrolyte arms. The scaling theory for the conformation of an individual polyelectrolyte star in the absence of the counterion condensation on the star arms as a function of the number of arms per star p and the fraction of charged segments f in an arm was developed by Borisov.[12] Three regimes have been identified for the star structure in a dilute solution: polyelectrolyte, osmotic, and quasi-neutral regimes. In section 3 we review the dilute regimes of polyelectrolyte stars and describe the phenomenon of counterion condensation on the star arms.

3. Dilute Solution of Polyelectrolyte Stars

3.1. Dilute Polyelectrolyte Regime, D_{PE}. In a dilute solution of stars, the distribution of counterions is determined by their interactions with the electric field of a star. The counterions remain free in solution if the electrostatic potential at the edge of the star is smaller than the thermal energy k_BT, i.e., when the entropy loss due to the confinement of a counterion within the volume of the star is larger than the gain of the energy of electrostatic interactions. Thus, the counterions are free in solution if the following condition is satisfied (up to logarithmic corrections due to the translational entropy at concentration c):

$$l_B \frac{pNf}{R} < 1 \tag{12}$$

where p is the number of arms per star, N is the number of Kuhn segments per arm, f is the fraction of charged segments, and R is the radius of the star. Below we show that this condition is stronger than the condition for preventing counterion condensation on the star arms. In other words, if the electrostatic field of a star does not influence the distribution of counterions, the field of each arm cannot change it either.

If the condition (eq 12) is fulfilled, the stars do not confine their counterions within their volume and the arms interact with each other via the unscreened Coulomb potential. The Coulomb interaction energy per arm in this regime of free counterions, called the polyelectrolyte regime, is

$$\frac{F_{Coul}}{k_BT} \approx l_B \frac{(pNf)^2}{pR} \tag{13}$$

This electrostatic repulsion stretches the arms and is balanced by the entropic elasticity of an arm

$$\frac{F_{str}}{k_BT} \approx \frac{R^2}{Nb^2} \tag{14}$$

so the equilibrium star radius in the polyelectrolyte regime increases as the cube root of the number of arms per star[12]

$$R_{PE} \approx bp^{1/3}N(uf^2)^{1/3} \tag{15}$$

The condition (eq 12) of no condensation of counterions within the star volume can be rewritten as

$$p\left(\frac{u^2 f}{p}\right)^{1/3} < 1 \tag{16}$$

The length scale characterizing the stretching of an arm due to the interarm repulsion is the tension blob size defined as the chain section having a tension energy on the order of k_BT[11,12,39]

$$\xi_t^{PE} \approx \frac{b^2 N}{R_{PE}} \approx \frac{b}{p^{1/3}}(uf^2)^{-1/3} \tag{17}$$

The tension blob defines the linear charge density $ef\xi_t^{PE}/b^2$ of a stretched arm (cf. eq 5), and according to eq 8 the counterions do not condense on the arms if

$$\left(\frac{u^2 f}{p}\right)^{1/3} < 1 \tag{18}$$

This condition is weaker than the condition (eq 16) for the polyelectrolyte regime of a star with the number of arms $p > 1$. Therefore, in the polyelectrolyte regime all counterions are free in solution and neither counterion condensation on the star nor on the arms occurs.

The polyelectrolyte regime has been considered in ref 12. It is realized for the stars with a few weakly charged arms (see eq 16)

$$p < p^* \approx (u^2 f)^{-1/2} \quad \text{for} \quad u^2 f < 1 \tag{19}$$

where p^* is the maximum number of arms which satisfies the condition (eq 12). This regime, however, is difficult to observe experimentally since it requires very weakly charged arms with $f < (pu)^{-2}$, which is typically less than 1 charge per 100 segments.

3.2. Dilute Osmotic Regime, D_{OS}. As the number of arms p or the charge fraction f increases, the arms become more stretched and the size of the tension blob correspondingly decreases (see eq 17). When ξ_t^{PE} is on the order of the distance between charges along the chain (when there is only one charge per tension blob), the free energy loss due to arm stretching becomes on the order of k_BT per charge, i.e., the same as the entropy gain per free counterion. At this point the counterions start to condense into the star volume indicating a crossover to the osmotic regime.

The counterions within the star volume can partially condense on the arms. In this case only fraction $\tilde{\beta}$ of the counterions is involved in the entropic contribution to the free energy of the star per arm

$$\frac{F_{OS}}{k_BT} \approx Nf\tilde{\beta}\ln\left(\frac{pNf\tilde{\beta}b^3}{R^3}\right) \tag{20}$$

The radius of the star R is determined by the balance of counterion entropy (eq 20) which favors the increase of the star volume and the entropic elasticity of arms given by eq 14 which opposes this expansion. Balance of these two contributions leads to the star radius

$$R_{OS} \approx bN(f\tilde{\beta})^{1/2} \tag{21}$$

and the tension blob size

$$\xi_t^{OS} \approx b(f\tilde{\beta})^{-1/2} \tag{22}$$

independent of the number of arms p. We ignore the weak logarithmic radial dependence of star arm stretching and the resulting logarithmic radial dependence of the size of the blob. Monte Carlo simulations of polyelectrolyte stars demonstrate that counterion distribution around an arm indeed has very weak radial dependence (see Figure 15 of ref 16).

Note that in the osmotic regime, the degree of localization of counterions in and near the star is optimized so that the contribution to the free energy of the star from counterion entropy is on the same order of magnitude as the electrostatic energy of a star reduced by localized counterions.

The fraction is estimated as

$$\tilde{\beta} \approx \frac{1}{u^2 f} \quad \text{for} \quad u^2 f > 1 \tag{23}$$

which is the same as the fraction β of free counterions in solution of individual chains (see eq 9). The counterions do not condense on the arms with low charge fraction $f < u^{-2}$ and this case ($\tilde{\beta} \approx 1$) corresponds to the osmotic regime considered in ref 12. The tension blob size and the length of the star arm in the osmotic regime depends on the value of the parameter $u^2 f$

$$\xi_t^{OS} \approx \begin{cases} bf^{-1/2}, & u^2 f < 1 \\ l_B, & u^2 f > 1 \end{cases} \tag{24}$$

$$R_{OS} \approx \begin{cases} bNf^{1/2}, & u^2 f < 1 \\ bNu^{-1}, & u^2 f > 1 \end{cases} \tag{25}$$

The size of the tension blob and the length of the arm in the regime of condensation on the arms are the same as the ones calculated for the linear chain (cf. eqs 10 and 11). This indicates that for $u^2 f > 1$, the arms of a star are not stretched relative to the size of an individual polyelectrolyte chain with counterions condensed on it.

The size of the star in the osmotic regime (eq 25) was obtained by the scaling arguments neglecting the radial dependence of the counterion distribution within the star. We have estimated that this r-dependence of the distribution of counterions is logarithmically weak and leads to the same results as the r-independent distribution with logarithmic accuracy. This estimate is in agreement with the results of simulations presented in ref 38 (see Table 2 therein).

To summarize, counterions do not condense on the star arms if the arms are weakly charged in a solvent with high dielectric permittivity ($u^2 f < 1$). The counterions are homogeneously distributed in solutions of sparsely branched stars ($p < (u^2 f)^{-1/2}$, polyelectrolyte regime) and are localized within the volume of the highly branched stars ($p > (u^2 f)^{-1/2}$,osmotic regime). In the opposite case ($u^2 f > 1$), the counterions condense on the arms and only fraction β of them (given by eq 9) participates in the osmotic contribution of the free energy of the star. Most of the uncondensed counterions are localized within the star with any number of arms p.

Note that scaling theories capture only the limiting cases of the counterion distribution. The broad crossover between these regimes is beyond the scope of the present paper where we mainly focus on the experimentally relevant osmotic regime with most of the counterions localized in and near the star.

An important remark has to be made regarding the electrostatic interactions of charged segments within a star in the osmotic regime. The radius of the star is proportional to the length of an arm (see eq 25) in both cases of counterion distribution around star arms. This dependence indicates that the electrostatic interaction of segments along an arm remains unscreened although most of the osmotically active counterions are localized in the close vicinity of the star reducing its net charge. We would like to stress again the difference between charge reduction by counterions and screening discussed at the end of the Introduction. Delocalization of a small fraction of counterions leads to an uncompensated charge of a star. The electrostatic energy of this uncompensated charge dominates over the energy of fluctuating gas of the counterions within the star making the screening by counterions in the osmotic regime impossible in the absence of salt.

3.3. Dilute Quasi-Neutral Regime, D_{QN}. In the center of the star, near the cross-linking point, the separation between arms is very small and the segment density is very high. The interarm separation r_{sep} at a distance r from the center is

$$r_{sep} \approx \frac{r}{p^{1/2}} \tag{26}$$

The dense packing of the segments extends up to the radial distance r_0 at which the arms are separated by the segment size b, i.e., the radius of the dense nucleus is equal to[5]

$$r_0 \approx bp^{1/2} \tag{27}$$

In the shell adjacent to the nucleus (at $r > r_0$) the segment concentration is still high, and the electrostatic interactions between charged segments are unimportant in comparison with the nonelectrostatic short-range interactions. The length scale of the short-range interactions between the segments belonging to different arms is on the order of the interarm separation (eq 26). We will refer to this shell as the quasi-neutral layer.[40] The structure of this layer can be thought of as a dense packing of the concentration blobs of the size r_{sep}.[5] In a θ-solvent, each arm follows the random walk statistics on the length scale smaller than the interarm separation.

Since the segment concentration within the star decreases with the radial coordinate, the role of the nonelectrostatic interactions diminishes and at a certain distance from the center, r_{QN} electrostatic interactions become dominant. The upper boundary of the quasi-neutral layer is determined by the condition that the interarm separation is on the order of the tension blob size (eq 24), so the size of the quasi-neutral layer is

$$r_{QN} \approx p^{1/2}\xi_t \approx \begin{cases} bp^{1/6}(uf^2)^{-1/3}, & \text{PE} \\ bp^{1/2}f^{-1/2}, & \text{OS for } u^2f < 1 \\ l_B p^{1/2}, & \text{OS for } u^2f > 1 \end{cases} \tag{28}$$

Thus, a highly branched star carrying a low charge could have a nucleus of the radius r_0 where the segments densely fill the space, a quasi-neutral layer ($r_0 < r < r_{QN}$) of concentration blobs (eq 26) and a more dilute outer part with stretched nonoverlapping arrays of the tension blobs[41] (see Figure 1).

In Figure 2 the radius R of the star (solid line) as well as the outer radius of the quasi-neutral layer r_{QN} (dashed line) are plotted as functions of the number of arms. In dilute polyelectrolyte regime (D_{PE}), the size of the star increases with increasing number of arms, p, faster than the size of its quasi-neutral layer. In the osmotic regime (D_{OS}), the size of the star does not depend on the number of arms (eq 21), while the size of the quasi-neutral layer increases (eq 28) and at $p \approx N^2f^2$ this layer occupies the whole volume of the star (the condition $r_{QN} \approx R_{OS}$ is fulfilled). This is an indication of the crossover to the quasi-neutral regime D_{QN}, where the radius of the star is no longer determined by the electrostatic interactions and is instead equal to[5]

$$R_{QN} \approx bp^{1/4}N^{1/2} \tag{29}$$

From Figure 2 one can see that extrapolations of solid and dashed lines can intersect at small values of p. Thus, decreasing the number of arms per star in the polyelectrolyte regime (D_{PE}) might cause a crossover to the second quasi-neutral regime. It happens if the charge density f is so low ($f < N^{-3/4}u^{-1/2}$) that each arm, taken as an individual chain, is not stretched by the intrachain electrostatic repulsion, and its conformation is the same as those of an uncharged chain (chain size is smaller than an electrostatic blob). In the present paper we will not consider such a case and assume that f is high enough that arms taken as isolated chains are larger than the size of an electrostatic blob.

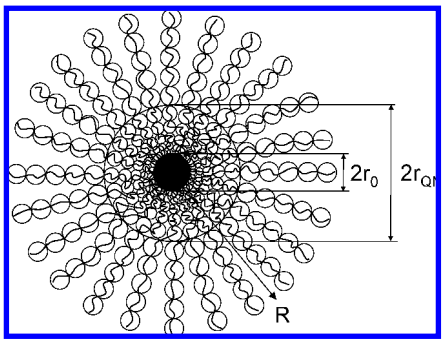

Figure 1. Schematic representation of the blob structure of a polyelectrolyte star. r_0 is the radius of a dense nucleus with a uniform concentration of segments. The shell $r_0 < r < r_{QN}$ consists of a dense packing of the concentration blobs. In the outer shell, $r > r_{QN}$, the arms can be represented as stretched arrays of the tension blobs.

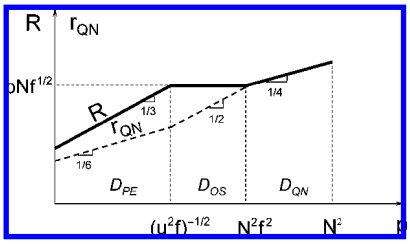

Figure 2. The radius of the star R (solid line) and the radius of the quasi-neutral layer, r_{QN}, (dashed line) as functions of the number of arms in a star, p, in the polyelectrolyte, D_{PE}, osmotic, D_{OS}, and quasi-neutral, D_{QN}, regimes.

The radius of the dense nucleus r_0 increases as the number of arms is increased (see eq 27). In the polyelectrolyte and osmotic regimes it is much smaller than the outer radius of the quasi-neutral layer and thus occupies a negligible part of the star volume. However, at a very large number of arms $p \approx N^2$, the radius of the dense nucleus is comparable with the radius of the whole star in the quasi-neutral regime (N^2 is the upper limit for the number of arms in a star in the present consideration).

4. Diagram of Regimes

In this section we describe the regimes of salt-free solutions of polyelectrolyte stars with different numbers of arms at different polymer concentrations. We consider both cases of counterion distribution around star arms. The diagrams in Figure 3 correspond to the case of uncondensed ($u^2f < 1$) and condensed ($u^2f > 1$) counterions, respectively.

4.1. Overlap Concentration. In dilute solutions the distance between the centers of mass of neighboring stars

$$R_{cm} \approx b\left(\frac{pN}{cb^3}\right)^{1/3} \tag{30}$$

is much larger than their radius. We define the star overlap concentration as concentration at which R_{cm} is on the order of the radius of the star R in dilute solution, so

$$c^* \approx \frac{pN}{R^3} \tag{31}$$

The overlap concentration c^* (eq 31) is the upper boundary of the dilute solution regime in the model.

The star overlap concentrations according to our definition (eq 31) for the regimes described in section 3 are compiled in Table 1 and shown in Figure 3a by the lines 1, 2, and 3 and in Figure 3b by the lines 2′ and 3′.

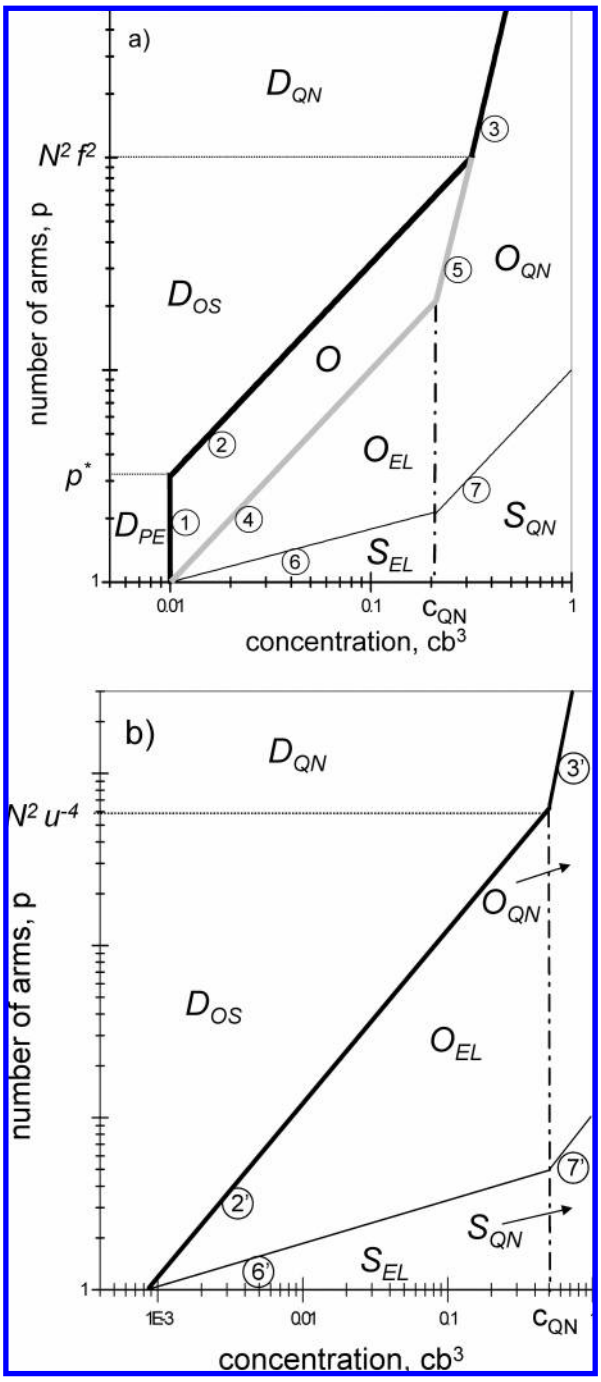

Figure 3. The diagram of different regimes of the solution of polyelectrolyte stars with p arms as a function of segment concentration, c (logarithmic scales): (a) for $u^2f < 1$, the values of the parameters are $N = 100$, $f = 0.1$, and $u = 1$; (b) for $u^2f > 1$, the values of the parameters are $N = 100$, $f = 1$, and $u = 2$. Different regimes (letters with subscripts) and crossover lines (numbers) are defined in the text.

4.2. Overlap Regimes. In solutions of linear polymers, the overlap is reached at a unique concentration. In solutions of stars it is expanded into a concentration range manifesting an existence of the regime where the stars remain at the onset of overlap without significant interpenetration. Below we justify the overlap regimes by studying the stretching of the star arms.

In the scaling analysis presented in section 3 we emphasized a considerable difference between the electrostatically dominated regimes with and without condensation of counterions on the star arms. The characteristic length of the interarm repulsion is the tension blob size (eqs 17 and 24). In the polyelectrolyte and osmotic regimes where the counterions do not condense on the arms ($u^2f < 1$), the tension blob size is smaller than the size of the electrostatic blob (eq 2) determined by the intra-arm stretching. This means that the repulsion between segments belonging to different arms is stronger than the repulsion between segments along the arm. As a result the extension of star arms is larger than the extension of individual linear polyelectrolyte chains. Contrary, in the osmotic regime where the counterions are condensed on the arms ($u^2f > 1$), the tension blob size is on the order of the electrostatic blob (eq 10) indicating that there is no additional stretching due to interaction between arms in a star.

Table 1. The Overlap Concentration c^* in Dilute Regimes of Salt-Free Solutions of Polyelectrolyte Stars

	c^*b^3
D_{PE}	$\frac{1}{N^2}(uf^2)^{-1}$
D_{OS}	$\frac{p}{N^2 f^{3/2}}$ $u^2f < 1$
	$\frac{pu^3}{N^2}$ $u^2f > 1$
D_{QN}	$\frac{p^{1/4}}{N^{1/2}}$

4.2.1. Regime O. In this section we consider solutions of stars with weakly charged arms in a solvent with high dielectric permittivity ($u^2f < 1$) corresponding to the condition for no counterion condensation on the star arms. The diagram of regimes as a function of polymer concentration c and number of arms in a star p is shown in Figure 3a. In a dilute solution up to the overlap concentration ($c \le c^*$), the star arms repel each other. Therefore, they are stretched in comparison with unconnected chains with the same number of segments and the same degree of charging. Above the overlap ($c > c^*$), this additional stretching of the arms makes an interpenetration of neighboring stars unfavorable as long as the interarm separation is much smaller than the correlation length of a semidilute solution of a linear polyelectrolytes ξ_{corr} at the same concentration c, see ref 42

$$\xi_{corr} \approx b(cb^3)^{-1/2}(uf^2)^{-1/6} \tag{32}$$

Stars shrink with increasing concentration reducing their stretching energy while maintaining the dense packing. This regime of overlap (regime O in Figure 3a) continues up to the concentration at which the interarm separation at the edge of the star becomes on the order of the correlation length ξ_{corr} (eq 32). A schematic sketch of the solution structure in the regime of overlap is shown in Figure 4. The size $R(c)$ of a star is comparable to the distance between neighboring stars.

The radius of the star at the higher concentration boundary of the overlap regime O, at $c = c^{**}_{EL}$, is given by (cf. eqs 26 and 32)

$$R(c^{**}_{EL}) \approx p^{1/2}\xi_{corr}(c^{**}_{EL}) \approx bp^{1/2}(c^{**}_{EL}b^3)^{-1/2}(uf^2)^{-1/6} \tag{33}$$

Throughout the whole regime of overlap and, therefore, at the crossover concentration c^{**}_{EL}, the stars are densely packed, so

$$c^{**}_{EL} \approx \frac{pN}{R^3(c^{**}_{EL})} \tag{34}$$

Substituting eq 33 into eq 34, we find the size of stars at the crossover concentration c^{**}_{EL}

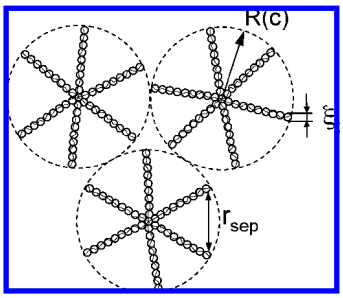

Figure 4. Schematic illustration of the solution structure in the overlap regime O of the diagram in Figure 3a. The star radius $R(c)$ is on the order of the distance between neighboring stars. The distance between arms r_{sep} is smaller than the correlation length of the corresponding semidilute polyelectrolyte solution at concentration c. The blob size ξ_t is smaller than the electrostatic blob size.

$$R(c_{EL}^{**}) \approx bN(uf^2)^{1/3} \tag{35}$$

which coincides with the size of a polyelectrolyte chain in a dilute solution with the same number of segments and degree of charging as one arm of a star (cf. eq 4). The tension blob size at $c = c_{EL}^{**}$ is equal to the size of the electrostatic blob (eq 2), and therefore the stretching of the arm is determined by the interaction of segments along the arm.

The concentration at the end of the regime O is estimated as (see eqs 34 and 35)

$$c_{EL}^{**}b^3 \approx \frac{p}{N^2}(uf^2)^{-1} \tag{36}$$

This boundary is shown by line 4 in Figure 3a.

Let us introduce the concentration-dependent tension blobs so that the star size is $R \approx \xi_t(c)N/g_t \approx b^2N/\xi_t(c)$, where the close packing condition implies $R \approx (pN/c)^{1/3}$. Therefore the tension blob size in the overlap regime is

$$\xi_t(c) \approx b\frac{N^{2/3}}{p^{1/3}}(cb^3)^{1/3} \tag{37}$$

It is increasing from its value in the dilute regime (eqs 17 or 22) to its value in the semidilute regime, electrostatic blob size ξ_{el} (eq 2).

In the regime of overlap O, the shrinking of the stars leads to an increase of the segment concentration inside the star. As a result the quasi-neutral central part of the star occupies larger volume. The radius of the quasi-neutral layer r_{QN} (eq 28) increases with concentration because of the increase of the tension blob size (eq 37)

$$r_{QN} \approx p^{1/2}\xi_t(c) \approx bp^{1/6}N^{2/3}(cb^3)^{1/3} \tag{38}$$

If r_{QN} becomes on the order of the radius of the whole star, $R(c) \approx R_{cm}$ (eq 30), i.e., at the concentration

$$c_{QN}^{**}b^3 \approx \frac{p^{1/4}}{N^{1/2}} \tag{39}$$

(line 5 in Figure 3a), the arms of a star interact exclusively via the short-range three-body repulsion. The interarm separation at the crossover concentration c_{QN}^{**} is equal to the correlation length of the semidilute solution of uncharged linear polymers ξ_{corr}^{θ} [39]

$$\xi_{corr}^{\theta} \approx b(cb^3)^{-1} \tag{40}$$

The concentration c_{QN}^{**} (eq 39) has the same expression as the overlap concentration c^* in the quasi-neutral regime D_{QN} (line 3 in Figure 3a).

The two different functional dependencies of the upper concentration boundaries of the overlap regime O on the parameters of the star solution c_{EL}^{**} (eq 36 and line 4 in Figure 3a) and c_{QN}^{**} (eq 39 and line 5 in Figure 3a) are explained by two different types of interactions cutting off this regime. The stretching of stars with few arms diminishes with concentration until it is controlled by the intra-arm electrostatic repulsion (to the right of line 4). The decrease of the electrostatic stretching in highly branched stars continues with concentration until this stretching becomes less important than the stretching due to the short-range nonelectrostatic repulsion (to the right of line 5).

Analysis of the diagram in Figure 3a allows us to evaluate the importance of the regimes for different values of the parameters such as N, f, and p. The dilute polyelectrolyte regime (D_{PE} in Figure 3a) is predicted for the number of arms $p < (u^2f)^{-1/2}$. For realistic values of the parameters this regime is very narrow. The dilute quasi-neutral regime (D_{QN} in Figure 3a) can be observable for the stars with short weakly charged arms with the number of charges per arm less than the square root of the number of arms $Nf < p^{1/2}$.

The concentration range at which the regime of overlap (O in Figure 3a) is predicted (the width of the regime) can be estimated from the ratio of the concentration c_{EL}^{**} to the overlap concentration c^* in the osmotic regime

$$\frac{c_{EL}^{**}}{c_{OS}^{*}} \approx \frac{1}{uf^{1/2}} \tag{41}$$

The concentration range of the overlap regime depends on the strength of the electrostatic interactions in solution: the regime is wider for smaller parameter u^2f.

4.2.2. Regimes O_{EL} and O_{QN}. In the previous section we considered the regime of overlap which is expected for the stars with arms electrostatically repelling each other. If the interarm electrostatic repulsion is screened, the length scale of interactions between arms is on the order of the correlation length in a semidilute solution of linear chains. Segment concentration within a star decreases with the radial coordinate; therefore, a part of a star further from the center becomes screened at a lower polymer concentration in solution than a part close to the center. The solution structure is characterized by an inhomogeneous polymer density distribution due to the existence of the cores where the arms are stretched by the interarm repulsion and the molten coronas where the interarm repulsion is screened (see the sketch in Figure 5). However, the core is much smaller than the distance between the centers of mass of the stars and its size is negligible as compared to the size of the corona. The size of the corona (same order of magnitude as the size of the arm) is dictated by the dense packing of the correlation blobs; hence, almost the whole solution can be thought of as a melt of correlation blobs. An important question here is whether the stars interdigitate upon an increase of polymer concentration or they compact as distinct nonoverlapping molecules.

Interdigitation requires that the size of a star R is larger than the distance between the centers of mass of neighboring stars R_{cm} which is determined solely by the polymer concentration. Consider the star size at a given concentration with and without interdigitation. If the stars do not interdigitate, all densely packed

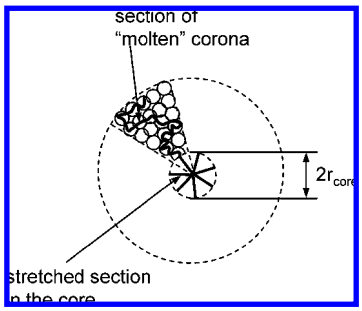

Figure 5. Schematic illustration of an arm conformation in the overlap regimes O_{EL} and O_{QN}. The radius of the core r_{core} where the arms are stretched is much smaller than the distance between neighboring stars. The radius of the whole star, which is on the order of the distance between neighboring stars, is determined by the size of the corona where the arm conformation is determined by a densely packed array of correlation blobs.

correlation blobs within R belong to the same star. Thus $R \approx R_{cm} \approx b(\tilde{N}p)^{1/3}$, where $\tilde{N}p$ is the total number of correlation blobs in a star ($\tilde{N}$ blobs per arm). With complete interdigitation, the arms from neighboring stars are indistinguishable. The solution represents the melt of arms, so the arm size is Gaussian $R_G \approx \tilde{N}b^{1/2}$.

As the concentration is increased, R_{cm} decreases and interdigitation may occur as R_{cm} reaches the Gaussian size of arms R_G. Thus, the condition for interdigitation is $R_G \approx R_{cm}$, so $(\tilde{N}p)^{1/3} \approx \tilde{N}^{1/2}$, or equivalently

$$\tilde{N} \approx p^2 \tag{42}$$

For single chains $p = 1$, so always $\tilde{N}^{1/2} > R_{cm} \approx \tilde{N}^{1/3}$ and interdigitation occurs immediately upon overlap. The arms of a star with $p \gg 1$ are stretched relative to the Gaussian size in a broad concentration range leading to the existence of the overlap regime without interdigitation.

Depending on the dominant interaction, two types of the overlap regime can be introduced. For the stars without counterions condensed on their arms ($uf^2 < 1$, Figure 3a), regime O_{EL} (dominated by the electrostatics) follows regime O at concentrations higher than c^{**}_{EL} (line 4 and eq 36). Regime O_{QN} (dominated by the nonelectrostatic interactions) is predicted above the concentration c^{**}_{QN} (line 5 and eq 39) and above the overlap concentration in the quasi-neutral regime (line 3). In the solutions of stars with strongly charged arms corresponding to the case of counterions condensed on the arms ($uf^2 > 1$, Figure 3b), the overlap regimes O_{EL} and O_{QN} are predicted above the overlap concentration in the regimes D_{OS} and D_{QN}, respectively.

The number of correlation blobs per arm $\tilde{N}$ depends only on polymer concentration and is not affected by possible interdigitation. It is estimated as $\tilde{N} \approx N/g_{corr} \approx Nb^2/(\xi_{corr}\xi_{el})$ using the relation between the correlation length ξ_{corr} and the number of segments g_{corr} in it, $\xi_{corr} \approx g_{corr}b^2/\xi_{el}$. In the electrostatically dominated regime, the correlation length is given by eq 32 for $u^2f < 1$ and in the case of counterions condensed on the arms (for $u^2f > 1$) the correlation length is

$$\xi^c_{corr} \approx b(cb^3)^{-1/2}u^{1/2} \tag{43}$$

According to the condition (eq 42), the crossover to the regime of interpenetration of stars in the semidilute electrostatically dominated regime (S_{EL}) is given by (see line 6 in Figure 3a and line 6′ in Figure 3b)

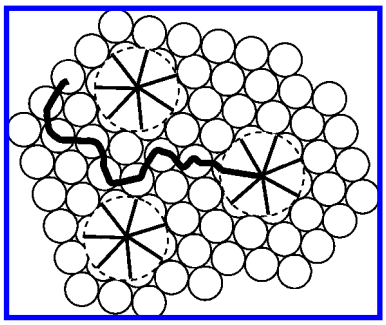

Figure 6. Schematic illustration of an arm conformation in the semidilute regime dominated by electrostatic interactions S_{EL}. The coronas of distant stars interpenetrate each other, and each arm has a conformation of a linear chain in a semidilute polyelectrolyte solution.

$$c^{***}_{EL}b^3 \approx \begin{cases} p^4N^{-2}(uf^2)^{-1} & \text{for } u^2f < 1 \\ p^4N^{-2}u^3 & \text{for } u^2f > 1 \end{cases} \tag{44}$$

At the concentration c_{QN}

$$c_{QN}b^3 \approx \begin{cases} (uf^2)^{1/3} & \text{for } u^2f < 1 \\ u^{-1} & \text{for } u^2f > 1 \end{cases} \tag{45}$$

(shown in Figure 3a,b by a vertical dash-dotted line), the size of the electrostatic blob (eqs 2 and 10) is equal to the correlation length given by eq 32 for $u^2f < 1$ and by eq 43 for $u^2f > 1$ and is also equal to the correlation length of a semidilute solution of uncharged polymers given by eq 40. Above c_{QN}, the electrostatic interactions are no longer important and the solution structure outside the small core region is the same as in the solution of uncharged stars.[7,9] The number of correlation blobs per arm in this regime is estimated as $\tilde{N} \approx N/g_{corr} \approx Nb^2/\xi^2_{corr}$ (where correlation length in this quasi-neutral regime is given by eq 40) and the crossover to the regime of interpenetration (semidilute quasi-neutral regime S_{QN}) is given by the following equation (see lines 7 and 7′ in parts a and b of Figure 3, respectively)

$$c^{***}_{QN}b^3 \approx pN^{-1/2} \tag{46}$$

4.3. Semidilute Regimes, S. Above concentrations c^{***} (see the thin solid lines 6 and 7 at the bottom of Figure 3a and 6′ and 7′ in Figure 3b and eqs 44 and 46), the cores are surrounded by the arms belonging to distant stars indicating that coronas of many stars interpenetrate (see Figure 6). The structure of the solution is approaching that of the semidilute solution of linear polyelectrolytes (S_{EL}) or linear uncharged chains (S_{QN}). The interarm interactions are screened due to the presence of other stars, and the correlation length is the same as in a semidilute solution of linear chains. In other words, the effect of the branch point and associated with it arm stretching is negligible in semidilute regimes (it is localized in a small core region around the branch point).

The size of an arm in the regime S_{EL} is on the order of the size of a linear chain with N segments and the fractional charge f in a semidilute solution at the same concentration

$$R^s_{lin} \approx \begin{cases} bN^{1/2}(cb^3)^{-1/4}(uf^2)^{1/12} & \text{for } u^2f < 1 \\ bN^{1/2}(cb^3)^{-1/4}u^{-1/4} & \text{for } u^2f > 1 \end{cases} \tag{47}$$

In the regime S_{QN}, the arm size is $bN^{1/2}$.

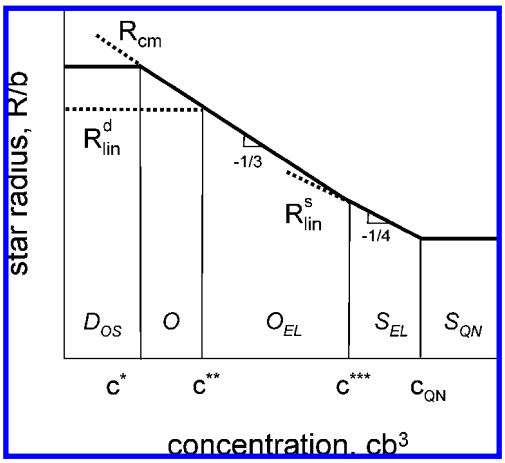

Figure 7. Schematic sketch of the dependence of the star radius R on the solution concentration c in the absence of counterion condensation on the arms ($u^2f < 1$, logarithmic scales).

Both electrostatically dominated and quasi-neutral semidilute regimes are predicted for stars with long arms: for larger N, these regimes extend to a larger number of arms p.

4.4. Concentration Dependence of the Star Radius. The diagram of regimes allows one to follow the variation of the star radius as a function of concentration as the star solution passes through its numerous regimes. Figure 7 demonstrates the dependence of the star radius R on the polymer concentration c ranging from a dilute solution to a melt. The dependence is plotted for the case $u^2f < 1$ starting from the dilute osmotic regime.

In a dilute regime, the star radius is much smaller than the distance between the centers of mass of the stars R_{cm} and it does not depend on concentration. Above the overlap concentration c^* there is a regime of overlap where the radius of the star decreases proportionally to R_{cm}. In the case of osmotic stars without counterion condensation on the arms, two consecutive regimes of overlap are present. In the regime O, the stars compact in order to reduce the stretching of the arms due to the interarm electrostatic repulsion. This regime continues until the arm stretching is equal to the stretching of a single polyelectrolyte chain in a dilute solution R^d_{lin}. In the overlap regime O_{EL}, the stretching decreases with concentration until the size of an arm becomes on the order of the linear chain size R^s_{lin} in a semidilute solution. In the case of stars with counterions condensed on the arms ($u^2f > 1$), only overlap regime O_{EL} is present. Finally the size of the star decreases similar to the size of linear chains in a semidilute solution (regime S_{EL}) and saturates at the ideal star size in regime S_{QN}.

5. Star Solutions in the Presence of Salt

5.1. Dilute Regimes. In a dilute salt-free solution of osmotically swollen stars, most of the counterions are localized within the volume occupied by the stars. The effective charge of a star is determined by a small fraction of delocalized counterions. Upon addition of a low-molecular weight salt, mobile ions partition themselves between the space inside and outside each star. Salt ions with the same charge sign as counterions are localized in the volume of a star in an excess amount in order to compensate the effective charge. We distinguish two limiting salt concentration regimes. If c_s is much lower than the concentration of counterions in the star, $c_{c-i} \approx pNf\beta/R^3$, the internal ion concentration c_{int} is on the order of counterion concentration ($c_{int} \approx c_{c-i}$ if $c_s \ll c_{c-i}$). The radius of the star R is determined by the osmotic pressure of the counterions. In the other limiting regime, the concentration of salt is much higher than the concentration of counterions ($c_s \gg c_{c-i}$) and the ion concentration inside the star is on the order of the concentration of salt in solution ($c_{int} \approx c_s$). At the crossover between these two regimes (at $c_s \approx c_{c-i}$), the effective charge of a star is completely compensated and the concentrations of ions inside and outside a star become approximately equal. Therefore, in the regime of high salt, the fluctuation energy of mobile ions dominates the interarm electrostatic energy and the osmotic contribution to the free energy becomes negligible. The size of a star in this regime is determined by the screened electrostatic interactions of charged segments.

The diagram of scaling regimes of salt solutions of stars is shown in Figure 8a for the case of no counterion condensation on star arms and in Figure 8b for the counterions condensed on the arms. If the salt concentration is lower than the crossover concentration

$$c_s^I b^3 \equiv \frac{pNf\beta b^3}{R_{OS}^3} \approx \begin{cases} pN^{-2}f^{-1/2} & \text{for } u^2f < 1 \\ puN^{-2} & \text{for } u^2f > 1 \end{cases} \quad (48)$$

the star radius is the same as in a salt-free solution given by eq 25. In the diagram, this salt-independent regime is denoted as D_{OS} (see Figure 8a,b). The star size at salt concentrations higher than the crossover value c_s^I is governed by the electrostatic interactions screened due to added salt (regime D_{SS} in Figure 8a,b). The radius of screening is equal to the Debye length

$$r_D \approx b(c_s b^3 u)^{-1/2} \quad (49)$$

The expression for the Debye radius at the crossover concentration c_s^I in the two cases of counterion distribution around star arms,

$$r_D|_{c_s=c_s^I} \approx \begin{cases} \dfrac{bNf^{1/2}}{p^{1/2}(u^2f)^{1/4}} \approx \dfrac{R_{OS}}{p^{1/2}(u^2f)^{1/4}} & \text{for } u^2f < 1 \\ \dfrac{bN}{up^{1/2}} \approx \dfrac{R_{OS}}{p^{1/2}} & \text{for } u^2f > 1 \end{cases} \quad (50)$$

indicates that at $c_s > c_s^I$, the screening radius is larger than the distance between arms in the case of no counterion condensation and it is smaller than that if counterions are condensed on the arms. In the former case, added salt screens the interactions between the arms, whereas in the latter case the interarm electrostatic interactions are already screened and additional salt screens the interactions between segments along one arm.

5.1.1. Regime of No Counterion Condensation on the Arms ($u^2f < 1$). The structure of a star in the regime of no counterion condensation was described in refs 31 and 32. Here we reconsider the description by introducing a new physical picture which allows one to follow the sequence of the regimes.

Since the screening radius r_D is larger than the distance between arms, several arms within r_D interact via unscreened electrostatic repulsion. The stretching of a section of each arm is determined by the balance of the energy of interarm Coulomb repulsion and the conformational entropy of the corresponding section of an arm. The arm section within the screening radius r_D at the edge of the star contains n monomers. There are $\tilde{p}$ such sections of different arms participating in the unscreened Coulomb interaction within the screening radius,

$$\tilde{p} \approx p\left(\frac{r_D}{R_{SS}}\right)^2 \quad (51)$$

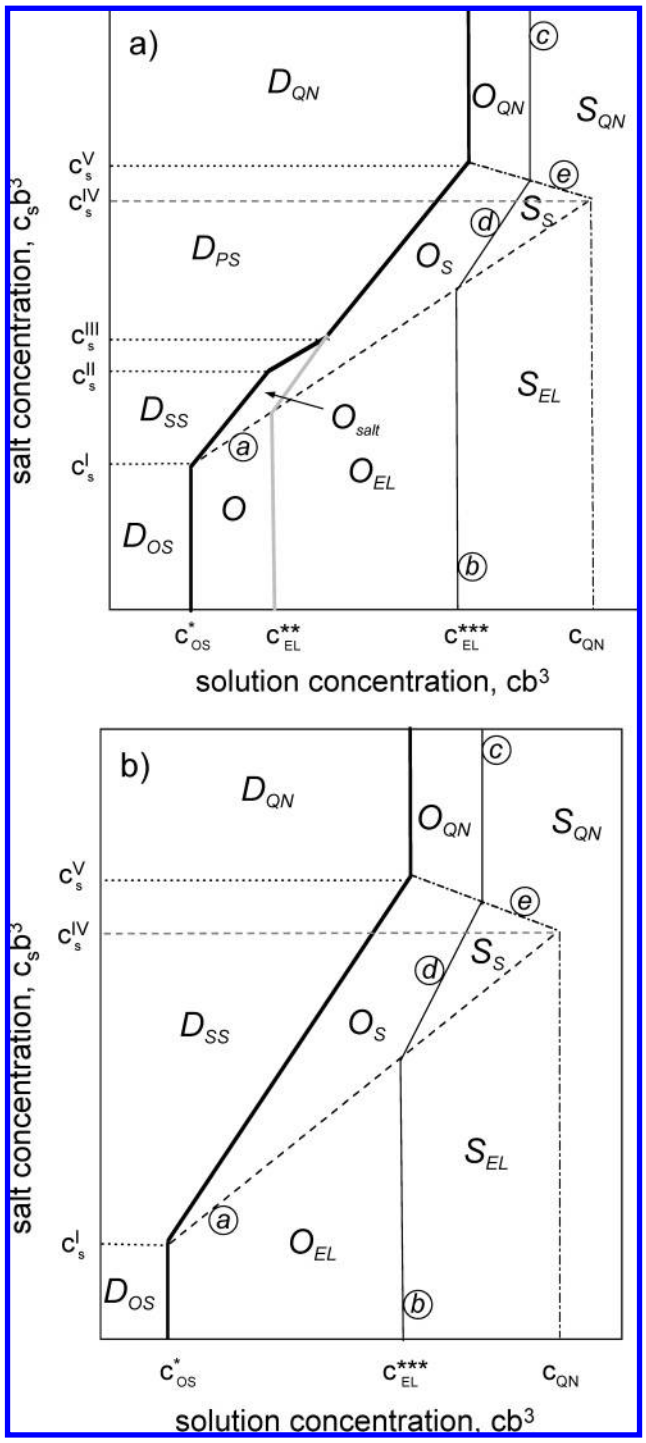

Figure 8. Schematic sketch of the diagram of different regimes of the solution of polyelectrolyte stars in the presence of salt as a function of segment concentration c and salt concentration c_s (logarithmic scales): (a) for $u^2f < 1$; (b) for $u^2f > 1$. Different regimes (upper case letters with subscripts) and crossover lines (lower case letters) are defined in the text.

where R_{SS} is the radius of a star in the regime D_{SS}. The electrostatic energy per single arm section containing n segments

$$\frac{\tilde{F}_{\text{Coul}}}{k_B T} \approx \frac{(\tilde{p}nf)^2 l_B}{\tilde{p} r_D} \tag{52}$$

is balanced by the stretching energy stored in this section

$$\frac{\tilde{F}_{\text{str}}}{k_B T} \approx \frac{r_D^2}{nb^2} \tag{53}$$

From eqs 52 and 53, one can self-consistently determine the number of monomers per section of the size r_D,

$$n_D \approx \frac{r_D \xi_{el}}{b^2 \tilde{p}^{1/3}} \quad \text{for} \quad u^2 f < 1 \tag{54}$$

The star can be considered as consisting of $p/\tilde{p}$ groups of arms. Within each group, the arms electrostatically interact on length scales smaller than the Debye radius r_D, while the interaction between different groups is screened. Thus, it can be represented by an effective star with $p/\tilde{p}$ arms each containing N/n_D segments of the size r_D interacting with each other via short-range repulsion (see Figure 9a). The size of this effective star is

$$R_{SS} \approx r_D \left(\frac{p}{\tilde{p}}\right)^{1/5} \left(\frac{N}{n_D}\right)^{3/5} \tag{55}$$

This expression can be rewritten in the form of the radius of a neutral star with p arms containing N segments each in a good solvent[5]

$$R_{SS} \approx b p^{1/5} N^{3/5} \left(\frac{\upsilon_{el}^D}{b^3}\right)^{1/5} \quad \text{for} \quad u^2 f < 1 \tag{56}$$

where

$$\frac{\upsilon_{el}^D}{b^3} \approx \frac{r_D^2 b}{\xi_{el}^3} \approx f^2 (c_s b^3)^{-1} \quad \text{for} \quad u^2 f < 1 \tag{57}$$

might be thought of as an effective excluded volume per segment originating from the screened interarm electrostatic repulsion. According to eq 56, addition of salt leads to a change of the statistics of an arm from $R \sim N$ (see eq 25) to $R \sim N^{3/5}$. (see eq 56).

As salt concentration increases, the Debye radius r_D decreases down to the distance between arms and at $c_s^{II} \approx pu/N^2(u^2f)^{4/3}$ the interarm repulsion at the edge of a star becomes completely screened. The sections of each arm in the outer shell of the star are stretched due to exclusive intra-arm electrostatic repulsion and have a conformation of a string of electrostatic blobs. Close to the center, however, the interarm repulsion remains unscreened because the Debye radius covers more than one arm. Thus, at $c_s > c_s^{II}$ a star is divided into two layers: in the inner layer the arms still repel each other within screening length r_D, whereas in the outer layer the interarm interaction is screened. The radius of the star at salt concentrations higher than c_s^{II} is determined by the radius of the inner part which decreases with increasing salt concentration as $r_D p^{1/2} \approx b(p/uc_s b^3)^{1/2}$.

The Debye length in the outer layer is smaller than the distance between arms, so the screening radius has to be recalculated to ensure the electroneutrality of the screening volume, i.e., the number of salt ions in the volume has to be on the order of the charge of the arm section inside the volume. It was shown[42] that in this case the screening radius can be estimated as

$$r_B \approx r_D (u^2 f)^{1/6} \tag{58}$$

This value is smaller than the Debye radius indicating that the charged polymer segments participating in a screening make

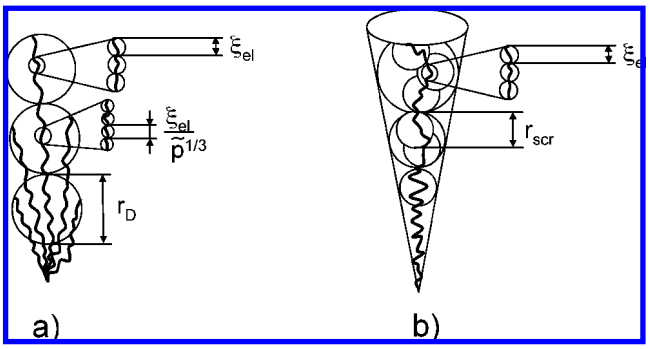

Figure 9. Schematic sketch of the blob structure of one arm in the regime of screening (a) by salt ions for $u^2f < 1$ and (b) by polymer segments for $u^2f < 1$ (the screening radius r_{scr} is equal to the radius r_B) and by salt ions for $u^2f > 1$ (the screening radius r_{scr} is equal to the Debye radius r_D).

the screening more effective. Sections of polyions behave as multivalent charges with shorter screening length than by that associated with monovalent counterions.

As the salt concentration is increased, the inner part becomes smaller while the outer layer grows. If the outer part constitutes most of the star, the crossover to a new regime occurs at the salt concentration c_s^{III} (see Figure 8a). We refer to the regime at higher salt concentrations ($c_s > c_s^{III}$) as to the regime of polymer screening and denote it by D_{PS} in Figure 8a.

In the regime D_{PS}, the conformation of an arm on length scales smaller than r_B is a string of electrostatic blobs, therefore the number of segments belonging to one arm within this screening radius r_B is

$$n_B \approx g_{el}\frac{r_B}{\xi_{el}} \approx \frac{r_B\xi_{el}}{b^2} \quad \text{for} \quad u^2f < 1 \tag{59}$$

On length scales larger than r_B, the conformation of an arm is a self-avoiding walk of screening radii r_B up to the distance between neighboring arms (see Figure 9b, where the screening radius r_{scr} is equal to r_B). The radius of the star in the regime D_{PS} is calculated as the radius of a neutral star with the arms containing N/n_B segments of the size r_B in an athermal solvent

$$R_{PS} \approx r_B p^{1/5}\left(\frac{N}{n_B}\right)^{3/5} \approx bp^{1/5}N^{3/5}\left(\frac{v_{el}^B}{b^3}\right)^{1/5} \tag{60}$$

where we introduced the effective excluded volume per segment originating from the intra-arm electrostatic interactions screened by polymer segments

$$\frac{v_{el}^B}{b^3} \approx \frac{{r_B}^2 b}{{\xi_{el}}^3} \approx \frac{f^2}{c_s b^3}(u^2f)^{1/3} \tag{61}$$

Note that this effective excluded volume v_{el}^B is smaller than v_{el}^D (eq 57) by the factor $(u^2f)^{1/3}$.

The crossover between the regimes D_{SS} and D_{PS} occurs at the salt concentration $c_s^{III} \approx pu/N^2(u^2f)^{14/9}$ at which the thicknesses of the inner and the outer layers are equal.

5.1.2. Regime of Counterions Condensed on the Arms ($u^2f > 1$). In the case of counterions condensed on the arms, the screening radius is equal to the Debye length which is smaller than the distance between arms at salt concentrations higher than c_s^I. In Figure 8b this regime is denoted as D_{SS} since the screening is governed by the salt. The structure of a star in this regime is similar to the structure of a star in the regime D_{PS} described in the previous section with the only difference that the electrostatic blob size is on the order of Bjerrum length (see eq 10). Therefore, the star radius is

$$R_{SS} \approx bp^{1/5}N^{3/5}\left(\frac{v_{el}^D}{b^3}\right)^{1/5} \quad \text{for} \quad u^2f > 1$$

where

$$\frac{v_{el}^D}{b^3} \approx \frac{{r_D}^2 b}{{\xi_{el}}^3} \approx u^{-4}(c_s b^3)^{-1} \quad \text{for} \quad u^2f > 1 \tag{62}$$

is an effective excluded volume per segment originating from the screened intra-arm electrostatic repulsion. The conformation of an arm is represented by a flexible chain of effective segments of the size r_D. On the length scale larger than r_D, conformation of an arm is a self-avoiding walk of the effective segments up to the distance between neighboring arms (see Figure 9b, where the screening radius r_{scr} is equal to r_D).

5.1.3. Crossover to the Quasi-Neutral Regime. Increasing salt concentration enhances the screening by decreasing the screening radius r_D (eq 49) for the case of counterions condensed on the arms and r_B (eq 58) for the case of no condensation. At the salt concentration higher than

$$c_s^{IV}b^3 \approx \begin{cases} f^{5/3}u^{1/3} & \text{for } u^2f < 1 \\ u^{-3} & \text{for } u^2f > 1 \end{cases} \tag{63}$$

(see the horizontal dashed line in Figure 8a,b), the screening radius is smaller than the electrostatic blob size. The electrostatic interaction between neighboring chain sections of the size ξ_{el} becomes screened, so that these sections electrostatically interact with the energy smaller than k_BT. To describe the structure of a star at $c_s > c_s^{IV}$, let us introduce a new length scale $\tilde{\xi}_{el}$ by the analogy with the thermal blob in a good solvent.[39] Chain sections of this size interact with each other with the energy on the order of k_BT. The size of this electrostatically induced thermal blob is

$$\tilde{\xi}_{el} \approx \begin{cases} \dfrac{b^4}{v_{el}^B} \approx b\dfrac{(c_s b^3)}{f^2}(u^2f)^{-1/3} & \text{for } u^2f < 1 \\ \dfrac{b^4}{v_{el}^D} \approx b(u^4 c_s b^3) & \text{for } u^2f > 1 \end{cases} \tag{64}$$

The conformation of an arm on length scales smaller than $\tilde{\xi}_{el}$ is a random walk of segments. On larger length scales ($r > \tilde{\xi}_{el}$), the arms follow the self-avoiding walk statistics up to the length scales on the order of distance between arms.

The size of the electrostatically induced thermal blob $\tilde{\xi}_{el}$ increases linearly with increasing salt concentration reflecting a weakening of electrostatic repulsion. At the salt concentration

$$c_s^V b^3 \approx \begin{cases} N^{1/2}f^{7/3}u^{2/3}/p^{1/4} & \text{for } u^2f < 1 \\ N^{1/2}/u^4p^{1/4} & \text{for } u^2f > 1 \end{cases} \tag{65}$$

$\tilde{\xi}_{el}$ is on the order of the distance between the arms. Above this crossover concentration, the structure of the star resembles that of a neutral star in a θ-solvent (regime D_{QN}, see section 3.3).

5.1.4. Salt Concentration Dependence of the Star Radius. In Figure 10 we plot the dependence of the star radius R on the added salt concentration c_s in a dilute solution of osmotically swollen stars. The dependence is plotted for the case of no counterion condensation on star arms ($u^2f < 1$). Two plateaus

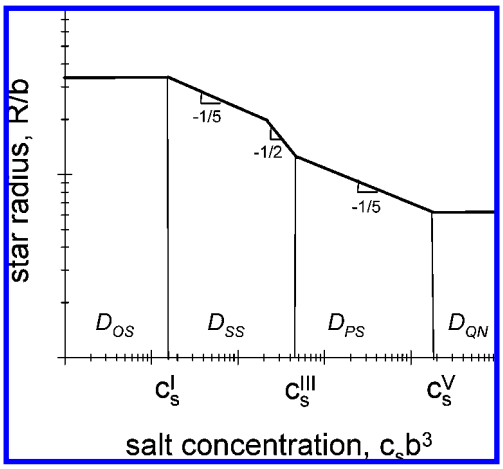

Figure 10. Schematic sketch of the dependence of the star radius R on the salt concentration c_s in the absence of counterion condensation on the arms ($u^2f < 1$, logarithmic scales).

at a very low and a very high salt concentration correspond to the regimes where the screening by salt is unimportant (D_{OS}) and where salt completely screens electrostatic interactions (D_{QN}), respectively. At moderate salt concentrations, the radius of stars decreases with c_s as $c_s^{-1/5}$ in a wide range over the two regimes D_{SS} and D_{PS}. The change of the slope in the regime D_{SS} from $-1/5$ to $-1/2$ occurs in a very narrow interval of salt concentrations which is estimated as $c_s^{III}/c_s^{II} \approx (u^2f)^{-2/9}$. The slope $-1/2$ of the salt concentration dependence of the star radius corresponds to the two-shell structure of the star with a large inner shell dominated by salt screening and a narrow outer shell dominated by polymer screening.

In the case of stars with counterions condensed on the arms ($u^2f > 1$), only salt-dominated regime D_{SS} is present.

5.2. Regimes of Overlap and Semidilute Regimes. Above the overlap concentration c^* (shown in Figure 8a,b by the thick solid lines), the stars are in the overlap regimes. The overlap regimes O, O_{EL}, and O_{QN} have been described in detail in section 4.2.2. The characteristics of these regimes are salt-independent. The effect of added salt is pronounced in the regimes O_{salt} (for the stars without counterions condensed on the arms, Figure 8a) and O_S (for both cases of counterion distribution around the arms). The physical principles explaining the appearance of the regime O_{salt} are the same as discussed for the regime O, while the regime O_S is similar to the regimes O_{EL} and O_{QN}. Quantitative differences are due to the nature of interactions between segments. They result in the salt concentration dependence of the star size and crossovers between the regimes. In Table 2 we have compiled the characteristics of the salt-dominated regimes for the two cases of counterion distribution around the arms. The structure of the solution in semidilute regime S_S resembles that of a semidilute solution of polyelectrolyte chains in the presence of salt.[42]

The crossover between the regimes of screening by salt (O_S and S_S) and the quasi-neutral regimes with completely screened electrostatic interactions (O_{QN} and S_{QN}) is introduced following the same procedure as in a dilute solution (see the previous section). Above the salt concentration c_s^{IV} (dashed horizontal line) where the screening radius becomes smaller than the size of the electrostatic blob, the conformation of an arm is described using a new length scale, the size of the electrostatically induced thermal blob $\tilde{\xi}_{el}$ (eq 64). At $c_s > c_s^{IV}$, the correlation length of the solution is calculated by the analogy with the correlation length in a solution of uncharged chains in a good solvent.[39]

$$\tilde{\xi}_{corr} \approx \begin{cases} b\left(\frac{b^3}{\upsilon_{el}^B}\right)^{1/4}(cb^3)^{-3/4} & \text{for } u^2f < 1 \\ b\left(\frac{b^3}{\upsilon_{el}^D}\right)^{1/4}(cb^3)^{-3/4} & \text{for } u^2f > 1 \end{cases} \quad (66)$$

The conformation of an arm on small length scales ($r < \tilde{\xi}_{corr}$) is a self-avoiding walk of electrostatically induced thermal blobs of size $\tilde{\xi}_{el}$. At salt concentration (shown by the dashed−dotted line e in the Figure 8a,b)

$$c_{QN}^S b^3 \approx \begin{cases} (c_s b^3)^{-1} f^2 (u^2 f)^{1/3} & \text{for } u^2f < 1 \\ (c_s b^3)^{-1} u^{-4} & \text{for } u^2f > 1 \end{cases} \quad (67)$$

the correlation length $\tilde{\xi}_{corr}$ (eq 66) becomes equal to the correlation length in the solution of uncharged chains in a θ-solvent ξ_{corr}^{θ} (eq 40) and at the same time to the size of the electrostatically induced thermal blob $\tilde{\xi}_{el}$ (eq 64). At higher salt concentrations, the radius of the star is salt-independent.

6. Discussion and Conclusions

In the present paper we have developed a scaling theory of solutions of polyelectrolyte stars. The theory includes two limiting cases of counterion distribution around the star arms. The counterions are condensed on the arms if $u^2f > 1$, where $u \equiv l_B/b$ is the ratio of the Bjerrum length to the Kuhn segment length and f is the fraction of charged Kuhn segments in an arm. The condition for the condensation is fulfilled in solutions with a low dielectric permittivity. In aqueous solutions where the typical value of u for flexible polyelectrolytes is $u \approx 2$, the counterions are condensed if the arms are sufficiently strongly charged ($f \approx 1$). The condensation leads to the decrease of the bare charge of an arm eNf down to the effective value $eNf\beta$, where β (eq 9) is the fraction of uncondensed counterions remaining entropically active. The effective charge of an arm, eN/u^2, is independent of the fraction of charged segments f, because an increase of the charge fraction is completely compensated by the condensation of counterions.[15]

If the counterions do not condense on the star arms, they are either free to move throughout the whole solution volume (polyelectrolyte regime) or they are localized within the volume of stars (osmotic regime). In the polyelectrolyte regime, charged polymer segments interact via Coulomb repulsion almost

Table 2. Characteristics of Salt-Dependent Regimes in Figure 8a,b, the Correlation Length ξ_{corr}^s, the Size of a Linear Chain in Semidilute Solution R_{lin}^s, and the Crossover Polymer Concentration to the Regime of Interdigitation $c_S^{***}b^3$ (Line e in Figure 8a,b)

	ξ_{corr}^s	R_{lin}^s/b	$c_S^{***}b^3$
$u^2f < 1$	$\frac{(c_sb^3)^{1/4}\xi_{el}}{(cb^3)^{3/4}}(u^2f)^{1/12}$	$\frac{N^{1/2}(uf^2)^{1/6}}{(cb^3)^{1/8}(c_sb^3)^{1/8}}(u^2f)^{-1/24}$	$\frac{p^{8/5}(c_sb^3)^{3/5}(uf^2)^{-12/5}}{N^{4/5}}(uf^2)^{1/5}$
$u^2f > 1$	$\frac{(c_sb^3)^{1/4}\xi_{el}^c}{(cb^3)^{3/4}}$	$\frac{N^{1/2}u^{-1/2}}{(cb^3)^{1/8}(c_sb^3)^{1/8}}$	$\frac{p^{8/5}(c_sb^3)^{3/5}u^{12/5}}{N^{4/5}}$

unaffected by counterions over all distances inside the star. Therefore, the star arms are stretched in comparison with linear polyelectrolyte chains carrying the same charge. In the osmotic regime, most of the counterions are localized within a volume of stars effectively reducing their charge to the value corresponding to the balance between the electrostatic attraction of a counterion to a star and the entropy of a counterion. The effective charge of a star is proportional to the number of delocalized counterions per star and is equal to ep^*Nf, where $p^* \approx (u^2 f)^{-1/2}$ is the number of arms at the crossover between the polyelectrolyte and osmotic regimes. The stretching of the arms is determined by the repulsion between the arms due to the effective charge. Since $p^* \gg 1$, the arms of a star in the osmotic regime are strongly stretched relative to linear polyelectrolytes.

The counterion condensation on the star arms changes essentially the structure of a dilute solution of stars. An electric field of a star with counterions condensed on its arms does not allow uncondensed counterions to leave the star. They are mostly localized within the volume of stars resulting in the same stretching of the arms as of unconnected linear polyelectrolytes.

The upper boundary of the dilute solution regime is the overlap concentration c^*. We define c^* as the concentration at which the distance between the centers of mass of neighboring stars is on the order of the size of a star in a dilute solution. In the paper by Borisov,[12] the overlap concentration was defined as the concentration at which the Debye screening radius due to counterions is on the order of the star radius. This definition is based on the assumption that the screening in solution is always determined by the Debye length. It was demonstrated, however, that this assumption fails in semidilute solutions[42] and, as we have shown in this paper, in dilute solutions with a high concentration of added salt.

Above the overlap concentration, we have identified the regimes which do not exist in solutions of linear chains. These regimes are intermediate between dilute concentrations where stars are far apart from each other and semidilute regimes where the stars are interdigitated and their arms interact as linear overlapping chains. In the concentration range above c^* and below the crossover to the semidilute regime, the radius of each star decreases with concentration in a way that stars remain in a space-filling noninterdigitated state. By analogy with the *overlap concentration* in solutions of linear chains we call this range of concentrations the *overlap regime.* The reason for star compaction prior to interdigitation is the stretching of star arms due to the interarm repulsion. This stretching has to disappear in order to make the interdigitation favorable.

There are two qualitatively different reasons for stretching of star arms, either due to long-range electrostatic interarm repulsion or due to short-range (either steric or screened electrostatic) repulsion. These two reasons for arm stretching lead to two qualitatively different overlap regimes, regime O (see Figure 3a) with long-range interarm repulsion (predicted only for stars without counterion condensation on arms) and regimes O_{EL} and O_{QN} (Figures 3a,b) with short-range repulsion expected for both types of counterion distribution near star arms.

In the case of stars without condensed counterions, the stretching of arms due to the long-range electrostatic interarm repulsion remains important above c^* as long as interarm separation is smaller than the electrostatic screening length. This overlap regime O continues with increasing polymer concentration until the long-range interarm electrostatic repulsion is screened and the stretching of the arm decreases to the one determined exclusively by the intra-arm repulsion.

The overlap regime determined by the short-range steric or screened electrostatic repulsion exists as long as the arms of star polymers are stretched preventing their interpenetration. This stretching is due to the packing constraint of having many arms attached to a single center of the star. Concentration blobs from all arms of a star at a given concentration densely pack into a sphere with a radius larger than the size of an unattached arm forcing arms to stretch. Blobs of a star pack into a denser sphere with a smaller radius at higher concentrations. At the crossover between overlap and semidilute regimes, the radius of the densely packed sphere of blobs becomes comparable to the size of an unattached arm and stars begin to interpenetrate.

Several microscopic models of interaction between polyelectrolyte stars have been studied in refs 17, 18, 43, and 44 with an emphasis on the interaction potential between pairs of stars. However, there is a qualitative difference between conformations of arms for a pair of stars compressed against each other in dilute solution (where arms can be deflected away from the approaching star) and for a star compressed from all sides by surrounding stars in a semidilute solution.

Addition of salt changes the structure of star solution in both dilute and semidilute regimes. We distinguish partial compensation of charges by counterions localized inside the star in the dilute osmotic regime from exponential screening of electrostatic interactions due to added salt. Electrostatic screening implies exponential decay of electrostatic interaction and requires electroneutrality of the screening volume, which is impossible in dilute solutions without salt because some counterions always escape from the volume of the star. We have analyzed the effect of added salt on the structure of an osmotically swollen star in a dilute solution and identified several regimes depending on salt concentration c_s. At very low salt concentrations, the screening by added salt is not important and the size of the star is almost the same as in a salt-free solution of osmotic stars. This salt-independent regime continues until the concentration of added salt increases up to the concentration of entropically active counterions inside the star. At higher salt concentrations, the electrostatic interactions between segments are screened by the salt and arm stretching weakens with c_s leading to a decrease of the star radius (see Figure 10).

In the case of no counterion condensation on the arms, the screening by salt begins on the length scale equal to the Debye radius r_D which is larger than the distance between arms but smaller than the size of a star. The stretching of the arms weakens both in tangential and in radial directions. Weakening of the stretching in the tangential direction is due to a decreased number of arms that interact via unscreened electrostatic repulsion. There are $\tilde{p} < p$ arms within the Debye radius, and their number decreases with increasing salt concentration c_s. A star can be thought of as containing $p/\tilde{p}$ bunches of $\tilde{p}$ electrostatically interacting arms. The bunches of arms follow self-avoiding walk statistics, and their radial size determines the radius of the star.

The interarm repulsion is completely screened at higher salt concentration at which the Debye length is comparable with or smaller than the interarm separation. The value of the screening radius in this regime is derived taking into account screening due to charged polymer segments (eq 58). This value is smaller than r_D indicating that the screening is enhanced by the polymer. The screening radius smaller than interarm separation leads to the screening of the intra-arm electrostatic repulsion. The arm can be represented by a sequence of effective segments with the size on the order of the screening radius. Within the screening radius, the conformation of an arm is a string of

electrostatic blobs, since the stretching is due exclusively to the intra-arm electrostatic repulsion. On length scales larger than the screening radius, the arm follows self-avoiding walk statistics. This structure is also found in the case of counterions condensed on star arms. In this case, the regime of screening begins when the Debye length is smaller than the distance between arms. A change of the arm statistics upon contraction of the star was analyzed by neutron scattering.[28] These measurements demonstrate that arms remain locally stretched at high salt concentrations, while their size follows excluded volume statistics. This observation is in agreement with the prediction of our model that an arm is stretched on length scales shorter than the screening radius and follows self-avoiding walk statistics on larger length scales.

The crossover to the regime where electrostatic interactions are totally screened is described by introducing a new length scale. This new length describes the conformation of an arm with the screening radius smaller than the size of the electrostatic blob. It is analogous to the thermal blob in neutral polymer solutions with excluded volume interactions, and we call it the electrostatically induced thermal blob. The size of this blob increases linearly with salt concentration and at some c_s becomes on the order of the interarm separation. At higher salt concentrations, the conformation of a star is the same as the conformation of an uncharged star in a θ-solvent determined by the short-range nonelectrostatic three-body repulsion between segments.

The overlap regimes in solutions of polyelectrolyte stars with added salt are analogous to the overlap regimes in salt-free solutions. The long-range interarm electrostatic repulsion in solutions of stars with no counterion condensation on the arms leads to the overlap regime O_{salt} (see Figure 8a) which is equivalent to the overlap regime O in salt-free solutions. The arms in the overlap regime O_{salt} remain stretched by long-range interarm repulsion until the Debye radius decreases to the distance between arms with increasing salt concentration. The short-range repulsion in solutions with both types of counterion distribution around the arms results in the overlap regime O_S (Figure 8a,b) similar to the overlap regimes O_{EL} and O_{QN} in salt-free solutions. The main difference between these regimes is that the interactions between charged monomers in the overlap regime O_S are screened by added salt.

Finally, let us discuss the experimentally testable predictions of our theory. We predict two cases of counterion distribution in the star solution: (i) counterions are localized within the volume of the star (spherical condensation); and (ii) a part of counterions localized in the star volume are condensed on the arms (linear condensation). The solution structure differs essentially for these two cases of condensation. In the case of linear condensation, the solution characteristics such as star radius, overlap concentration, and osmotic pressure do not depend on the degree of charging of the arms, as opposed to the case of spherical condensation. This property can be tested experimentally.

We predict the dependence of the radius of individual stars on solution concentration (see Figure 7) with the extended regime of overlap, where the stars do not interdigitate. According to our findings, the width of this regime increases with decreasing parameter $u \equiv l_B/b$. In the experimental work of refs 22 and 23, the authors investigated micelles with a frozen core and charged corona which are equivalent to polyelectrolyte stars. They found that above the physical overlap, the micelles shrink and start to interdigitate at concentrations essentially higher than the overlap concentration. Such experiments are the first step to systematic investigation of the overlap regime. Earlier, Muller et. al[20] used SANS to show that there are two scattering peaks at concentrations much higher than the overlap concentration. The position of one of these peaks changes with concentration c as $c^{1/3}$, while the position of the other varies as $c^{1/2}$. The first peak is related to the correlation between the stretched central parts of stars, and its position is inversely proportional to the distance between their centers of mass. The range of concentration where this peak is observed is associated with the overlap regime. The second peak appears at higher concentrations and is attributed to the correlations found in solution of linear polyelectrolytes;[21] therefore, the solution is in the semidilute regime.

An important characteristic of dilute star solutions with added salt is the dependence of star radius on salt concentration (see Figure 10). Although the physics of solution regimes is different for the two cases of counterion distribution around the arms, the c_s-dependence of the star radius is the same. It starts with a plateau at low c_s, then the radius decreases as $c_s^{-1/5}$ and finishes again with a plateau at high c_s. The main difference between the predictions of our theory and earlier results of Borisov and Zhulina[31,32] is the existence of the $c_s^{-1/2}$ regime due to shorter screening radius (r_B instead of r_D). The dependence $c_s^{-1/5}$ has been observed experimentally and reported in ref 28. Stronger ionic strength dependence ($c_s^{-1/2}$), however, has not been reported, most probably because this dependence is predicted for a very narrow salt concentration range. We are looking forward to further experimental tests that will provide more information about the unique properties of polyelectrolyte stars.

Acknowledgment. We are thankful to Dr. E. Zhulina for reading a preprint of the manuscript and providing constructive criticism. We would like to acknowledge financial support of National Science Foundation under Grants CHE-0616925 and CTS-0609087, National Institutes of Health under Grant 1-R01-HL0775486A, and NASA under Agreement NCC-1-02037.

References and Notes

(1) Riess, G. *Prog. Polym. Sci.* **2003**, *28*, 1107.
(2) Napper, D. H. *Polymeric Stabilization of Colloidal Dispersions*; Academic Press: London, U.K., 1985.
(3) Tadmor, R.; Janik, J.; Klein, J.; Fetters, L. J. *Phys. Rev. Lett.* **2003**, *91*, 115503-1.
(4) Bhatia, S. R.; Mourchid, A.; Joanicot, M. *Curr. Opin. Colloid Interface Sci.* **2001**, *6*, 471.
(5) Daoud, M.; Cotton, J. P. *J. Phys. France* **1982**, *43*, 531.
(6) Witten, T. A.; Pincus, P. A.; Cates, M. E. *Europhys. Lett.* **1986**, *2*, 137.
(7) Birshtein, T. M.; Zhulina, E. B.; Borisov, O. V. *Polymer* **1986**, *27*, 1078.
(8) Adam, M.; Fetters, L. J.; Graessley, W. W.; Witten, T. A. *Macromolecules* **1991**, *24*, 2434.
(9) Marques, C. M.; Izzo, D.; Charitat, T.; Mendes, E. *Eur. Phys. J. B* **1998**, *3*, 353.
(10) de Gennes, P.-G. *Scaling Concepts in Polymer Physics*; Cornell University Press: Ithaca, NY, 1979.
(11) Pincus, P. *Macromolecules* **1991**, *24*, 2912.
(12) Borisov, O. V. *J. Phys. II France* **1996**, *6*, 1.
(13) Heinrich, M.; Rawiso, M.; Zilliox, J. G.; Lesieur, P.; Simon, J. P. *Eur. Phys. J. E* **2001**, *4*, 131.
(14) Oosawa, F. *Polyelectrolytes*; M. Dekker: New York, 1970.
(15) Manning, G. S. *J. Chem. Phys.* **1969**, *51*, 924.
(16) Roger, M.; Guenoun, P.; Muller, F.; Belloni, L.; Delsanti, M. *Eur. Phys. J. E* **2002**, *9*, 313.
(17) Jusufi, A.; Likos, C. N.; Lowen, H. *Phys. Rev. Lett.* **2002**, *88*, 018301.
(18) Jusufi, A.; Likos, C. N.; Loven, H. *J. Chem. Phys.* **2002**, *116*, 11011.
(19) Wolterink, J. K.; Leermakers, F. A. M.; Fleer, G. J.; Koopal, L. K.; Zhulina, E. B.; Borisov, O. V. *Macromolecules* **1999**, *32*, 2365.
(20) Muller, F.; Delsanti, M.; Auvray, L.; Yang, J.; Chen, Y. J.; Mays, J. W.; Deme, B.; Tirrel, M.; Guenoun, P. *Eur. Phys. J. E* **2000**, *3*, 45.
(21) Essafi, W.; Lafuma, F.; Williams, C. E. *Eur. Phys. J. B* **1999**, *9*, 261.

(22) Korobko, A. V.; Jesse, W.; Egelhaaf, S. U.; Lapp, A.; van der Maarel, J. R. C. *Phys. Rev. Lett.* **2004**, *93*, 177801-1.
(23) Korobko, A. V.; Jesse, W.; Lapp, A.; Egelhaaf, S. U.; van der Maarel, J. R. C. *J. Chem. Phys.* **2005**, *122*, 024902-1.
(24) Hariharan, R.; Biver, C.; Russel, W. B. *Macromolecules* **1998**, *31*, 7514.
(25) Tanford, Ch. *Physical Chemistry of Macromolecules*; John Wiley & Sons Inc.: New York, 1961.
(26) Guenoun, P.; Muller, F.; Delsanti, M.; Auvray, L.; Chen, Y. J.; Mays, J. W.; Tirrel, M. *Phys. Rev. Lett.* **1998**, *81*, 3872.
(27) Förster, S.; Hermsdorf, N.; Böttcher, C.; Lindner, P. *Macromolecules* **2002**, *35*, 4096.
(28) Muller, F.; Guenoun, P.; Delsanti, M.; Deme, B.; Auvray, L.; Yang, J.; Mays, J. W. *Eur. Phys. J. E* **2004**, *15*, 465.
(29) Guenoun, P.; Schlachli, A.; Sentenac, D.; Mays, J. W.; Benattar, J. J. *Phys. Rev. Lett.* **1995**, *74*, 3628.
(30) Ahrens, H.; Förster, S.; Helm, C. A. *Phys. Rev. Lett.* **1998**, *81*, 4172.
(31) Borisov, O. V.; Zhulina, E. B. *Eur. Phys. J. B* **1998**, *4*, 205.
(32) Borisov, O. V.; Zhulina, E. B. *Macromolecules* **2002**, *35*, 4472.
(33) Schiessel, H.; Pincus, P. *Macromolecules* **1998**, *31*, 7953.
(34) Increasing the valence of counterions leads to increasing strength of electrostatic interactions and the appearance of correlation-induced attraction that would significantly modify our predictions. Counterion-correlation-induced attraction in solutions of linear polyelectrolytes was described in a recent publication, Liao, Q.; Dobrynin, A. V.; Rubinstein, M. *Macromolecules* **2006**, *39*, 1920.
(35) de Gennes, P. G.; Pincus, P.; Velasco, R. M.; Brochard, F. *J. Phys.* **1976**, *37*, 1461.
(36) Grosberg, A. Yu.; Khokhlov, A. R. *Statistical Physics of Macromolecules*; American Institute of Physics: New York, 1994.
(37) Deshkovski, A.; Obukhov, S.; Rubinstein, M. *Phys. Rev. Lett.* **2001**, *86*, 2341.
(38) Jusufi, A. *J. Chem. Phys.* **2006**, *124*, 044908.
(39) Rubinstein, M.; Colby, R. H. *Polymer Physics*; Oxford University Press: New York, 2003.
(40) The dielectric permitivity ϵ is assumed to be constant throughout the solution. The decrease of ϵ in the dense regions of the star might cause a formation of ionic pairs which would influence the structure and boundaries of these regions.
(41) Shusharina, N. P.; Nyrkova, I. A.; Khokhlov, A. R. *Macromolecules* **1996**, *29*, 3167.
(42) Dobrynin, A. V.; Colby, R. H.; Rubinstein, M. *Macromolecules* **1995**, *28*, 1859.
(43) Denton, A. R. *Phys. Rev. E* **2003**, *67*, 011804.
(44) Wang, H.; Denton, A. R. *J. Chem. Phys.* **2005**, *123*, 244901.

MA0711442